

Ectopic expression of the ATP synthase β subunit on the membrane of PC-3M cells supports its potential role in prostate cancer metastasis

WEI LI¹, YULIN LI¹, GAIYUN LI¹, ZILONG ZHOU¹, XIAONA CHANG¹,
YANG XIA², XINJIE DONG³, ZHIJING LIU¹, BO REN¹, WEI LIU⁴ and YILEI LI¹

¹The Key Laboratory of Pathobiology, Ministry of Education, The College of Basic Medical Sciences, Jilin University, Changchun, Jilin 130021; ²Department of Pathology, The Second Clinical Hospital, Jilin University, Changchun, Jilin 130021; ³Department of Pathology, The First Clinical Hospital, Jilin University, Changchun, Jilin 130021; ⁴Department of Pathology, Longgang District Central Hospital of Shenzhen, Shenzhen, Guangdong 518116, P.R. China

Received November 4, 2016; Accepted December 20, 2016

DOI: 10.3892/ijo.2017.3878

Abstract. Metastatic prostate cancer is associated with high mortality rates. Identification of metastasis-related proteins may facilitate the development of novel therapies for the treatment of metastatic disease. In the present study, we aimed to identify prostate cancer metastasis-associated membrane proteins. We developed a phage-displayed 7-mer peptide library to screen the target peptides that were specifically bound to PC-3M cells with subtractive panning from normal prostate cells and PC-3 prostate cancer cells. A novel short peptide (B04) was found to have high affinity to highly metastatic PC-3M cells. ATP synthase β subunit (ATP5B) was then identified as a binding partner of B04 on the PC-3M cell surface. ATP5B was expressed on the PC-3M cell membrane and on highly malignant human prostate cancer specimens, as shown using multiple methodologies. Furthermore, ATP5B-positive gold particles were detected on the cellular and mitochondrial membranes by immunoelectromicroscopy. These results implied the possibility that ATP5B may translocate from the inner mitochondrial membrane to the outer surface of PC-3M cells. Additional analysis showed that incubation of B04 with PC-3M cells reduced the detection of ATP5B by western blotting and flow cytometry and significantly inhibited the proliferation, invasion and metastasis of PC-3M cells. In conclusion, ATP5B, as a binding partner of a metastasis-related short peptide (B04) on prostate cancer cells, is involved in promoting prostate cancer metastasis. In

conclusion, ATP5B may be a promising biomarker and therapeutic target for highly metastatic malignancies.

Introduction

Distal metastasis of tumors is the main cause of mortality in patients with cancer. Invasion and metastasis are regarded as important factors in the assessment of malignant behavior of tumors and have been extensively examined in the field of cancer research (1-3). Prostate cancer, the most common type of cancer in the male urinary and reproductive system, is difficult to treat after the occurrence of local invasion and distal metastasis. Moreover, few targets associated with metastasis and malignancy have been identified. Therefore, elucidation of the novel mechanisms of prostate cancer metastasis and identification of potential targets for the diagnosis and treatment of highly malignant prostate cancers are needed.

Proteomics-based technologies are currently used for the large-scale analysis of proteins expressed in cells and tissues (4). These methods represent effective tools for the identification of tumor-associated antigens, particularly for identifying cellular membrane antigens (5,6). For example, in our previous study, we analyzed the differential protein expression in PC-3M cells and PC-3 cells using two-dimensional liquid phase chromatographic fractionation followed by matrix-assisted laser desorption/time-of-flight mass spectrometry (MALDI-TOF/MS) (unpublished data). ATP synthase and caveolin were found to be upregulated in highly metastatic PC-3M cells compared with low less metastatic PC-3 cells using additional bioinformatics analysis.

F1Fo-ATP synthase, which is exclusively localized in the inner membrane of the mitochondria, catalyzes the rate-limiting step of ATP formation in eukaryotic cells. However, more evidence has shown that F1Fo-ATP synthase is ectopically expressed on the plasma membrane of tumor cells and some types of normal cells, such as endothelial cells and adipocytes (7). Proteomic analysis of membrane fractions has indicated that some highly malignant cell types show higher ectopic expression of ATP synthase than less malignant

Correspondence to: Professor Yilei Li, The Key Laboratory of Pathobiology, Ministry of Education, The College of Basic Medical Sciences, Jilin University, Changchun, Jilin 130021, P.R. China
E-mail: liyl@jlu.edu.cn

Key words: prostate cancer, ATP synthase β subunit, metastasis, PC-3M cells, membrane proteins

cells (8,9). Ectopic ATP synthase, including ATP synthase beta subunit (ATP5B), is localized on lipid rafts or caveolae of the cytoplasmic membrane (10-12). However, the mechanisms responsible for the transport of this protein have not been established, and it is unclear how ectopic ATP5B promotes the invasion and metastasis of prostate cancer.

Accordingly, in the present study, we analyzed the localization and expression of ATP5B in PC-3M cells and explored the effects of this protein on the biological behavior of PC-3M cells in order to determine its role in the metastasis of prostate cancer.

Materials and methods

Cell lines and cell culture. PC-3 human prostate cancer, PC-3M highly metastatic human prostate cancer, and normal prostate cells (American Type Culture Collection, Manassas, VA, USA) were cultured in F12, RPMI-1640, or H-DMEM, respectively, supplemented with 10% fetal bovine serum (FBS), 100 U/ml penicillin and 100 mg/ml streptomycin (Amresco, Solon, OH, USA). The cell lines were grown as adherent monolayer cultures at 37°C with 5% CO₂ in a humidified incubator. Human paraffin-embedded prostate cancer tissue specimens (T4, N0, M0 and G1) were obtained from the Pathology Department of the Jilin University.

Subtractive bio-panning *in vitro*. PC-3M and PC-3 cells were used as positive target cells, whereas normal prostate cells were used as negative absorber cells. Normal prostate cells were grown to log phase, washed three times with phosphate-buffered saline (PBS), and blocked with 1% bovine serum albumin (BSA) for 30 min at 37°C. Approximately, 2x10¹¹ pfu phages were incubated with normal prostate cells at 37°C for 30 min with gentle agitation. After incubation, the supernatant containing unbound phages was incubated with blocked PC-3 cells at 37°C for 30 min with gentle agitation. Then, the supernatant containing unbound phages was incubated with blocked PC-3M cells at 37°C for 30 min with gentle agitation. The PC-3M cells were washed three times with 0.1% PBST (PBS plus 0.1% Tween-20, v/v) to remove the unbound phages. Phages bound to the cell membrane were then eluted with 1 ml of 0.2 M glycine (pH 2.2) for 15 min on ice and immediately neutralized with 200 µl of 1 M Tris-HCl (pH 9.1). The eluted phages were amplified, purified and titrated according to the manufacturer's instructions. Subsequently, 2x10¹¹ pfu phages were subjected to the next round of bio-panning.

Enzyme-linked immunosorbent assay (ELISA). PC-3M and PC-3 cells were seeded into 96-well plates (1x10⁴ cells/well). The cells were washed twice and fixed with 4% paraformaldehyde for 20 min at room temperature. A solution of H₂O₂ (3%, 100 µl/well) was added, and the plates were placed at room temperature for 30 min to inhibit endogenous peroxidase activity. The cells were then blocked with 5% BSA at 4°C overnight. The phages were added to PC-3M and PC-3 cells (3x10¹¹ pfu, 100 µl/well) and incubated at 37°C for 2 h. After washing with 0.5% TBST three times, the cells were incubated with 200 µl of mouse anti-M13 monoclonal antibodies (1:5,000; Santa Cruz Biotechnology, Santa Cruz, CA, USA) at 37°C for 1.5 h. Next, cells were washed three times with 0.1%

TBST and then incubated with 200 µl horseradish peroxidase (HRP)-labeled goat anti-mouse antibody IgG (1:5,000; Santa Cruz Biotechnology) at 37°C for 1 h. After washing three times with 0.1% TBST, the cells were incubated with 100 µl TMB at 37°C for 10 min, and the reaction was then terminated by adding 200 µl of 2M H₂SO₄. The absorbance was then measured at 450 nm using an ELISA plate reader. Cell-free wells were used as controls.

DNA sequencing of the positive phage clones. The selected positive phage clones were used to extract DNA for sequencing analysis. First, 65 µl polyethylene glycol (PEG)/NaCl was added to 200 µl phages at room temperature for 10 min. The mixture was then centrifuged at 12,000 rpm for 10 min at 4°C. The precipitate was suspended in iodide buffer [10 mM Tris-HCl (pH 8.0), 1 mM EDTA and 4 M NaI], followed by ethanol precipitation at room temperature for 10 min. Single-stranded DNA (ssDNA) was recovered and dissolved in TE buffer [10 mM Tris-HCl (pH 8.0) and 1 mM EDTA]. DNA sequencing of the selected phages was carried out by Sangon Biotech Co., Ltd. (Shanghai, China). The primer used for sequencing was -96 gIII 5'-CCCTCATAGTTAGCGTAACG-3'.

Cell immunofluorescence assay. PC-3M and PC-3 cells were cultured on coverslips overnight. One group of cells was then incubated with 2x10¹¹ pfu phages at 37°C for 8 h, washed three times with TBS, and fixed with 4% paraformaldehyde for 20 min at room temperature. Cells were then blocked in 5% BSA for 1 h at 37°C and incubated with mouse anti-M13 monoclonal antibodies (1:250), anti-ATP5B antibodies (1:200; Santa Cruz Biotechnology) and anti-E-cadherin antibodies (1:200; Santa Cruz Biotechnology) at 4°C overnight. After washing three times with PBS, the cells were then incubated with anti-mouse Alexa Fluor 488 (1:600; Cell Signaling Technology, Danvers, MA, USA) or anti-rabbit Alexa Fluor 555 (1:600; Cell Signaling Technology) at 37°C for 30 min. Cells were then washed three times with PBS, nuclei were stained with Hoechst 33342 and the slides were observed using a laser scanning confocal microscope (LSCM).

Affinity chromatography and liquid chromatography tandem mass spectrometry (LC-MS/MS) analyses. MS and LC-MS/MS analyses were employed to detect and identify the corresponding target proteins of the identified short peptide binding to ATP5B (B04). Sephrose-4B was pre-incubated with B04, and the Sephrose-4B coupled with B04 was incubated with membrane proteins of PC-3M cells for 1 h to obtain the corresponding B04-binding proteins. The eluted proteins were identified by LC-MS/MS analyses. LTQ Velos was used with the search database ipi.HUMAN.v3.53 protein database. The filter parameters for SEQUEST results were as follows: charge, +1 and Xcorr, ≥1.9; charge, +2 and Xcorr, ≥2.2; charge, +3 and Xcorr, ≥3.75; DelCN, 0.1. The MS/MS data, including the mass values, intensity and charge of the precursor ions, were analyzed with the Mascot 2.0 against the Swiss-Prot protein database.

Immunoelectromicroscopy. The cells were fixed with 4% paraformaldehyde at 4°C for 20 min and washed in PBS three times. Cells were then incubated with 5% BSA for 1 h, and

the primary anti-ATP5B antibody (diluted 1:100) was applied at 4°C overnight. After three 5-min washes with PBS, and cells were incubated with the secondary antibody (goat anti-mouse) labeled with gold colloid (Wuhan Boster Biological Technology, Ltd., Wuhan, China) at room temperature for 1 h. Cells were washed in PBS three times, and immune complexes were pelleted by centrifugation (3,000 rpm for 5 min). The suspensions were mixed with an equal volume of 3% phosphotungstic acid (pH 7.0) placed on formvar-coated, carbonized copper grids and observed under a transmission electron microscope (TEM; Phillips 201; Norelco, Eindhoven, The Netherlands).

Flow cytometric analysis. PC-3M cells were fixed with 4% paraformaldehyde for 15 min and then washed twice with staining buffer. Cells were then blocked with 5% BSA in PBS and incubated with antibodies against ATP5B for 45 min at 4°C after washing twice. Secondary antibodies (Alexa Fluor 488 rabbit anti-mouse IgG [H+L]) were used at a 1:500 dilution for 30 min at 4°C. The stained cells were then analyzed using a flow cytometer (Becton-Dickinson, Franklin Lakes, NJ, USA). The percentage of cells was documented using ModFit software (Becton-Dickinson).

Western blotting. Cells were lysed with RIPA lysis buffer containing 1 mM phenylmethylsulfonyl fluoride (PMSF; Beyotime Institute of Biotechnology, Shanghai, China) on ice for 30 min. Total cellular proteins were assayed using a BCA kit (Beyotime Institute of Biotechnology). Equal amounts of protein were subjected to sodium dodecyl sulfate polyacrylamide gel electrophoresis (SDS-PAGE) and then electrophoretically transferred to polyvinylidene fluoride (PVDF) membranes. Membranes were blocked with 5% non-fat dry milk in PBS with 0.1% Tween-20 for 1 h at 37°C and the incubated with anti-ATP5B, anti-B04, anti-β-actin and anti-GAPDH antibodies at 4°C overnight. Finally, membranes were incubated with HRP-conjugated secondary antibodies for 1 h. The signals of detected proteins were visualized on an enhanced chemiluminescence (ECL; Beyotime Institute of Biotechnology) western blotting detection system (Amersham Biosciences, Inc., Piscataway, NJ, USA).

Cell Counting kit-8 (CCK-8) assays. PC-3M cells were seeded in 96-well plates at 1×10^4 cells/well in triplicate and incubated with B04 or 08K (as a control) for 6, 12, 24 or 48 h. After incubation, cells were detected using CCK-8 assays. Twenty microliters of CCK-8 solution was added to each well. The absorbance was measured at 450 nm to determine the number of viable cells in each well. All procedures were performed in triplicate.

Transwell assays. Cell invasion were analyzed using Transwell assays. The upper chambers were coated with 60 μl Matrigel (dilution 1:8), and 3×10^4 cells were then seeded in the upper chamber of each well in serum-free medium containing B04 or 08K. Additionally, 600 μl of RPMI-1640 media supplemented with 10% fetal calf serum (FCS) was added to the lower chamber. The cells were incubated for 24 h, after which the cells on the upper side of the filter were removed by wiping with a cotton swab. The cells that had invaded to

the lower surface were fixed with 4% paraformaldehyde and stained with Hoechst 33342. The average number of invaded cells was determined by counting the cells in 10 random fields (magnification, x100). Three independent experiments were performed with triplicate wells.

Tumor metastasis assay. Chicken embryo chorioallantoic membranes (CAMs) were used to explore the effects of B04 on the migration of PC-3M. PC-3M cells were cultured with B04 or 08K for 24 h as previously described. Cells were detached from the culture dish with 2 mM EDTA in PBS, counted, resuspended in 50 ml of PBS with Ca^{2+} and Mg^{2+} and inoculated (10^5 - 10^6 cells) onto the CAM of a 9-day-old chick embryo in which an artificial air sac was created (13). After 50 h of incubation, the lower half of the CAM was removed, placed in a sterile 14-ml polypropylene tube, snap-frozen in liquid nitrogen and stored frozen at -80°C. The frozen tissue was crushed in lysis buffer with sterile 5-ml pipettes. Genomic DNA was isolated from the lower CAMs using a DNA Isolation kit (Genra Systems, Inc., Big Lake, MN, USA) according to the manufacturer's specifications. The specific primers for human Alu sequences were as follows: Alu sense, 5'-ACGC CTGTAATCCCAGCACTT-3' and Alu antisense, 5'-TCGCC CAGGCTGGAGTGCA-3', which produced a band of 220 bp. The primers were positioned in the most conserved areas of the Alu sequence (14), with the first monomer at nucleotides 21-40 and the second monomer at nucleotides 263-245. Polymerase chain reaction (PCR) was performed according to the following conditions: 95°C for 2 min, followed by 30 cycles of 95°C for 30 sec, 63°C for 30 sec and 72°C for 30 sec. The reaction mixture contained 1 μg of genomic DNA as a template, 1X PCR buffer, 1.5 mM MgCl_2 , 50 μM dNTPs, 1.0 μM each of Alu sense and antisense primers, 1 ± 2 U of AmpliTaq Gold, and 0.1 μCi fresh ^{32}P -α-dCTP. The PCR products were electrophoresed on a 7% polyacrylamide gel at 100 V for 1 h, dried and exposed to film at -80°C. The bands were quantified by densitometric scanning using a Gel Scan XL (Pharmacia Biotech, Uppsala, Sweden).

Statistical analysis. All data were summarized as the mean ± standard deviations (SDs) from at least three independent experiments. Statistical analysis was performed using the SPSS Statistics 21. Differences between the means were analyzed using t-tests and one-way analysis of variance (ANOVA). A two-tailed $P < 0.05$ was considered statistically significant.

Results

Selection and identification of the phage clone B04 specifically bound to the membrane proteins expressed on PC-3M cells. Phages that specifically bound to PC-3M cells were identified through three rounds of *in vitro* subtractive bio-panning with PC-3 cells and normal prostate cells. In each round, a series of phages binding to the PC-3M cells instead of control cells was obtained and amplified for subsequent panning. The unbound phages were removed by washing with PBST. Fourteen positive phages were significantly selected and enriched (B01-14). The phage subtractive panning procedure is shown in Fig. 1. The 14 positive phage clones were selected for DNA

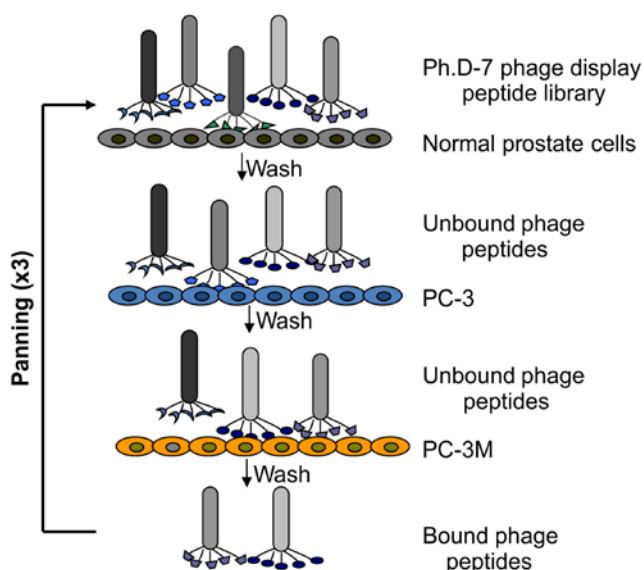


Figure 1. Procedures for phage subtractive panning. The Ph.D.-7 phage display peptide library was incubated with normal prostate cells to allow binding. The unbound phages were collected, incubated with PC-3 cells, collected again and incubated with PC-3M cells. After binding and eluting, the bound phages were amplified and subjected to three rounds of panning to enrich the peptides specifically binding to PC-3M cells.

Table I. Peptide sequences of positive phage clones.

Phage clone	DNA (21 bp)	Peptides
B01	GCTCCTCATTGCTTCGTCCT	APHLLRP
B02	TTTCGGGGGCTGGAGAGTGGT	FRGLESG
B03	ACGCGTATGGATCTGAAGTTG	TRMDLKL
B04	TGTGGTTGGACTCCGGTTATT	CGWTPVI
B05	GGGACTGCGACTCATCCTACG	GTATHPT
B06	ACTCCGAAGTATGATAATCAT	TPKYDNH
B07	TCGCCGACGTGGAGTTTTTTG	SPTWSFL
B08	TCTGGTTGGACTCCGGTTATT	SGWTPVI
B09	GGTACTAAGCTTACTTCTTTT	GTKLTSF
B10	AATGCTCCGGTTATTTTGCTT	NAPVILL
B11	AATCCGCCTTTGCTTACGCAT	NPPLLTH
B12	ACGCCGCCTCCTTTTAGGATT	TPPPFRI
B13	ACTTTTCGTTTGATGACTGAT	TFRLMTD
B14	GCGGTTAGTCGTGATATGCGT	AVSRDMR

The 14 positive phage clones were selected for DNA sequencing. Fourteen peptide sequences were obtained and named B01-14.

sequencing. The peptide sequences were then deduced from the DNA sequences. The 14 peptides were then designated B01-14 (as shown in Table I). The amino acid sequences of the 14 peptides were further analyzed and compared with the known proteins. B04 and B08 shared a common amino acid sequence: GWTPVI. Similar amino acid sequences, i.e., TP and PVI, had higher occurrence rates. Similar sequences were identified by Clustal W and National Center of Biotechnology Information BLAST analysis between the peptides displayed

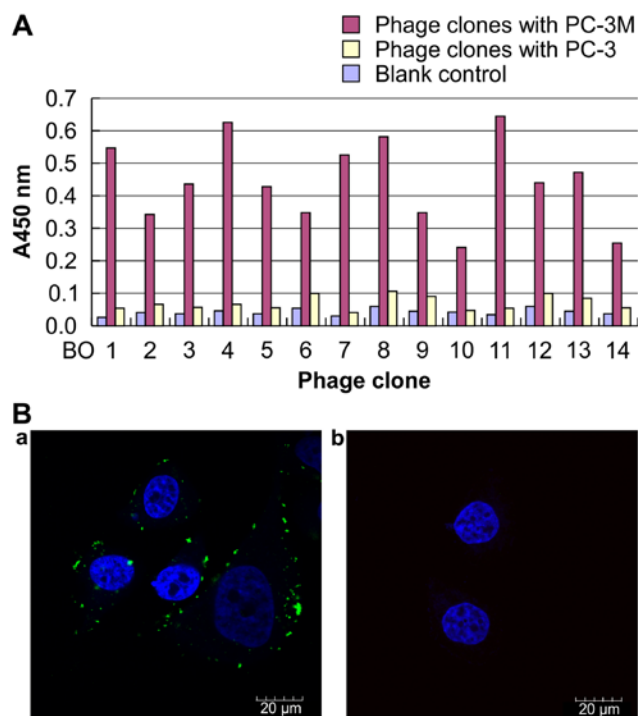


Figure 2. Specific binding of the selected positive phage clones to PC-3M cells. (A) Detection of the binding of positive phage clones (B01-14) to PC-3M and PC-3 cells using cellular ELISAs. PC-3 cells were used as a negative control. Wells with no cells were used as the blank control. (B) Immunofluorescence staining of PC-3M (a) and PC-3 (b) cells with B04 (a and b, magnification, $\times 2000$). B04-specific binding the cell membrane of PC-3M cells. The cell nuclei are shown in blue (Hoechst 33342) and B04 is shown in green.

by the phages and known proteins. The results showed that the peptides had the same sequences as 32 species of vascular endothelial cell surface proteins (data not shown), suggesting that highly metastatic prostate cancer may exhibit unique protein expression and molecular mechanisms to facilitate interactions with vascular endothelial cells.

Cellular ELISA and immunofluorescence assays were performed to determine the affinities of the 14 phage clones to PC-3M cells. The results of ELISA demonstrated that the 14 peptides specifically bound to PC-3M cells but not to PC-3 cells. B04, B08 and B11 peptides showed the highest binding ability to PC-3M cells (Fig. 2A). Immunofluorescence assays confirmed these findings (Fig. 2B). We chose the corresponding phage clones B04 and B08 (with the most consensus sequences) for further identification. Here, we focus on the results of B04. B04 was further confirmed to bind specifically with the cell surface proteins of PC-3M cells by immunofluorescence analysis (Fig. 2B-a), however, specific binding of B04 were not observed on the cellular surface of PC-3 cells (Fig. 2B-b). Therefore, the short peptide B04 was used as a hypothetical ligand for screening of metastasis-related proteins on the surface of PC-3M cells.

B04 binds to ATP5B on PC-3M cells. First, we extracted the plasma proteins and cellular membrane proteins from PC-3M cells and used B04 as the primary antibody to identify B04-binding proteins by western blotting. The results indicated that a specific 60-kDa protein from the cellular membrane fraction of PC-3M cells bound to B04; no bands were observed

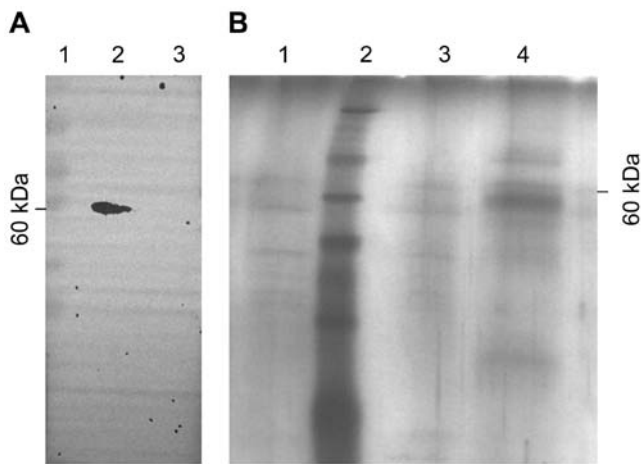


Figure 3. Binding of PC-3M membrane proteins to B04. (A) Western blot analysis of the target binding protein of B04. B04 was used as a primary antibody, and the black arrow p60 indicates the target protein of B04. Lane 1, marker; lane 2, membrane proteins of PC-3M cells; lane 3, plasma proteins of PC-3M cells. (B) PC-3M membrane p60 proteins binding to B04 were detected by silver staining. Sephrose-4B was pre-incubated with B04, and the Sephrose-4B coupled with B04 was then incubated with membrane proteins of PC-3M cells to obtain the corresponding B04-binding proteins. The flow-through fraction, wash fractions, and elution fractions were separated by SDS-PAGE and gels were visualized by silver staining. Lane 1, flow-through fraction; lane 2, marker; lane 3, wash fractions; lane 4, elution fractions.

from the plasma fraction of PC-3M cells (Fig. 3A). These data were consistent with the results of cell immunofluorescence assays (Fig. 2B).

Next, we confirmed these findings using affinity chromatography after pre-incubation of Sephrose-4B with B04. The Sephrose-4B used for coupling with B04 was incubated with cellular membrane proteins of PC-3M cells. The flow-through fraction, wash fractions and elution fractions were separated by SDS-PAGE and visualized by silver staining. A specific band of 60 kDa was found in the eluate, whereas no significant bands were found in the flow-through fraction or the wash fractions (Fig. 3B). The results above indicate that B04 bound to a protein with a molecular weight of 60 kDa on the PC-3M cell membrane.

Therefore, the p60 band was excised from the gel and further analyzed by MALDI-MS. Ten proteins were consistently identified in each of three independent experiments (Table II).

Taken together, these findings of immunofluorescence analysis, western blotting and MS confirmed that there was a protein expressed on the cell membrane of PC-3M cells that bound to B04. After excluding housekeeping proteins and plasma proteins, ATP5B was identified as the final B04-target protein.

ATP5B is expressed on the extracellular surface of PC-3M cells. We used immunofluorescence analysis to examine the expression and localization of ATP5B on PC-3M cells. As shown in Fig. 4A, ATP5B was found to be localized both on the cellular membrane and in the cytoplasm of PC-3M cells. However, positive staining was only found in the cytoplasm of PC-3 cells. Thus, we next performed immunoelectron microscopy to further define the localization of ATP5B on

Table II. MALDI-TOF-MS/MS analysis of 60-kDa peptides.

Protein	No. of amino acids	Molecular weight (kDa)	Transmembrane domain
ALB	609	66	Transmembrane protein
HSPA5	654	71	
SLC25A5	298	32.7	
ACTB			
TUBA1C	451	49.6	
GAPDH			
EEF1G	487	53.5	
EEF1A2			
ATP5B	529	58.1	Transmembrane protein
TRAP1	704	77.5	

PC-3M cells using gold particles (Fig. 4B). From the results of transmission electron microscopy (TEM), gold particles were detected both on the cellular membrane and in the cytoplasm of PC-3M cells, indicating expression on organelle membranes. The distribution of gold particles on the cellular membrane of PC-3M cells was detected on microvilli (Fig. 4B-a) and on the smooth surface of the cells (Fig. 4B-b). The gold particles were distributed on microvilli at a much higher frequency than that on the smooth surface of the cells; this phenomenon may be associated with the increased energy demand in highly metastatic tumor cells. However, no gold particles were observed on the cellular membrane of PC-3 cells (Fig. 4B-c and -d). We further investigated the surface localization of ATP5B in prostate cancer tissues using double immunofluorescence staining of ATP5B and E-Ca with paraffin-embedded prostate cancer tissue specimens. The expression of the ATP5B was obviously positive on the cellular membrane of prostate carcinoma specimens (Fig. 4C).

Next, we used flow cytometry to further confirm the presence of extracellular ATP5B on PC-3M cells with anti-ATP5B antibodies. ATP5B was present on the surface of PC-3M cells, and the percentage of ATP5B-positive cells and the fluorescence intensity of ATP5B were significantly higher in PC-3M cells than in PC-3 cells (61.68 ± 3.94 vs. $20.23 \pm 1.81\%$, respectively, for the percentage of ATP5B-positive cells; 53.87 ± 5.14 vs. 17.65 ± 0.19 , respectively, for the fluorescence intensity; Fig. 4D, $P < 0.05$). To further confirm the localization of ATP5B on the cellular membrane of PC-3M cells, plasma proteins and membrane proteins were separated from PC-3M and PC-3 cells, and anti-ATP5B antibodies were used to detect the expression of ATP5B in these fractions. The results indicated that ATP5B was expressed on the cellular membrane of PC-3M cells and that the expression ratio of ATP5B on PC-3M cells was significantly higher than that on PC-3 cells (Fig. 4E; $P < 0.05$). From the above results, we concluded that ATP5B was ectopically expressed on the cellular membrane of PC-3M cells.

Reduction of membrane-bound ATP5B levels inhibit proliferation, invasion and metastasis of PC-3M cells. ATP5B is

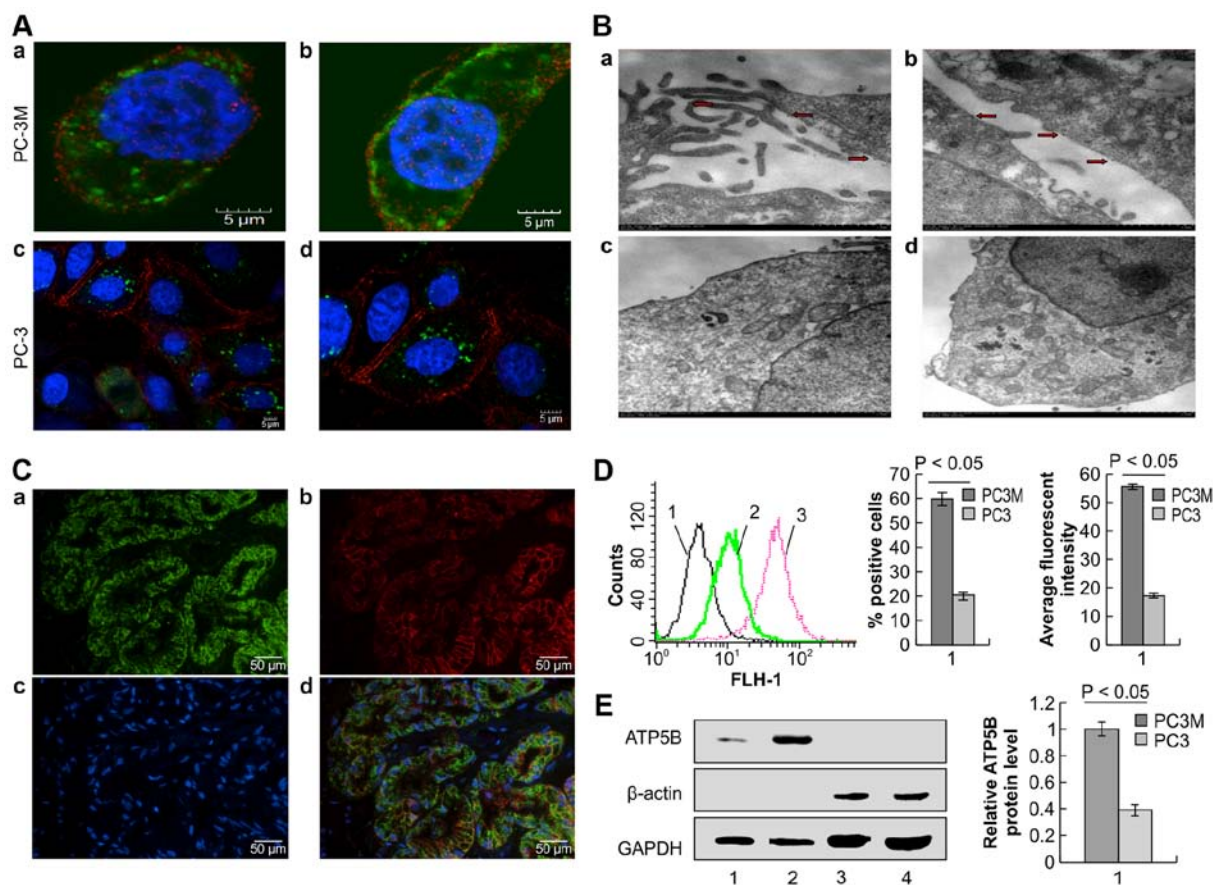


Figure 4. Subcellular localization of ATP5B. (A) Immunofluorescence localization of the ATP5B on the surface of PC-3M cells by confocal microscopy. Cells were stained with anti-ATP5B and anti-E-Ca antibodies, followed by secondary antibody staining. Non-permeabilized PC-3M cells are shown in a and b (magnification, x3000), and non-permeabilized PC-3 cells are shown in c (magnification, x1500) and d (magnification, x2000). ATP5B (green), E-Ca (red), and nuclei (blue) are shown. (B) Immunostaining of PC-3M cells with anti-ATP5B antibodies by immunoelectron microscopy. Gold particles on the cellular membrane are indicated by red arrows. (C) Immunocytochemistry double staining of ATP5B and E-Ca using paraffin-embedded tissue specimens. a, ATP5B (green); b, E-Ca (red); c, nuclei (blue); d, merged image of a-c. Magnification, x200. (D) Flow cytometric analysis of the localization of ATP5B. 1, PC-3M and PC-3 cells incubated with Alexa Fluor 488 IgG; 2, PC-3 cells incubated with antibodies against ATP5B; 3, PC-3 cells incubated with antibodies against ATP5B. (E) Western blotting was used to detect ATP5B expression. Lane 1, membrane proteins expressed in PC-3 cells; lane 2, membrane proteins expressed in PC-3M cells; lane 3, plasma proteins expressed in PC-3 cells; lane 4, plasma proteins expressed in PC-3M cells. GAPDH and β -actin were used as references for cellular membrane proteins and plasma proteins, respectively.

generally localized to the inner mitochondrial membrane where it functions to catalyze the rate-limiting step of ATP formation in eukaryotic cells (15). Our above-described results suggest that ATP5B partially translocated to the cellular membrane of PC-3M cells. Next, we investigated the potential functions of ectopically expressed ATP5B on the cellular membrane of PC-3M cells. First, we examined the spreading ability of PC-3M cells pre-incubated with B04 at different concentrations for 48 h. As shown in Fig. 5A, the impact of B04 on PC-3M cell spreading was concentration-dependent; higher concentrations of B04 resulted in greater inhibition of cell spreading. Moreover, CCK-8 assays indicated that B04 inhibited the proliferation of PC-3M cells *in vitro* (Fig. 5B). Cell growth curves showed that cell proliferation was significantly inhibited by B04 as compared with that in the control group.

Based on these results, we examined whether the anti-proliferative effects of B04 were caused by induction of cell cycle arrest through analysis of the cell cycle distribution. The results showed that B04 significantly affected the cell cycle distribution, leading to cell cycle arrest at the G2/M phase; the

percentage of cells in the G2/M phase increased from 9.91% in control cells to 34.28% in B04-treated cells. A corresponding decrease in the percentage of cells in the S phase was also observed (Fig. 5C).

In Transwell assays (Fig. 5D), we found that the invasive ability of PC-3M cells incubated with B04 was significantly decreased compared with that of PC-3M cells alone and PC-3M cells incubated with the control phage 08K ($P < 0.01$). In addition, the results of analysis with the CAM model showed that B04 significantly inhibited tumor metastasis, with an inhibition ratio of 23.41% (Fig. 5E), compared with that in the 08K group.

The above results demonstrated that B04 could effectively inhibit the aggressive properties of PC-3M cells, including proliferation, spreading, migration and invasion, i.e., the characteristic malignant behavior of highly metastatic tumors. To further confirm the role of specific binding of B04 with ectopically expression ATP5B on the cellular membrane of PC-3M cells in the inhibition of the malignant behavior, we used competitive inhibition experiments with B04 and anti-ATP5B antibodies. The results showed that ectopic expression

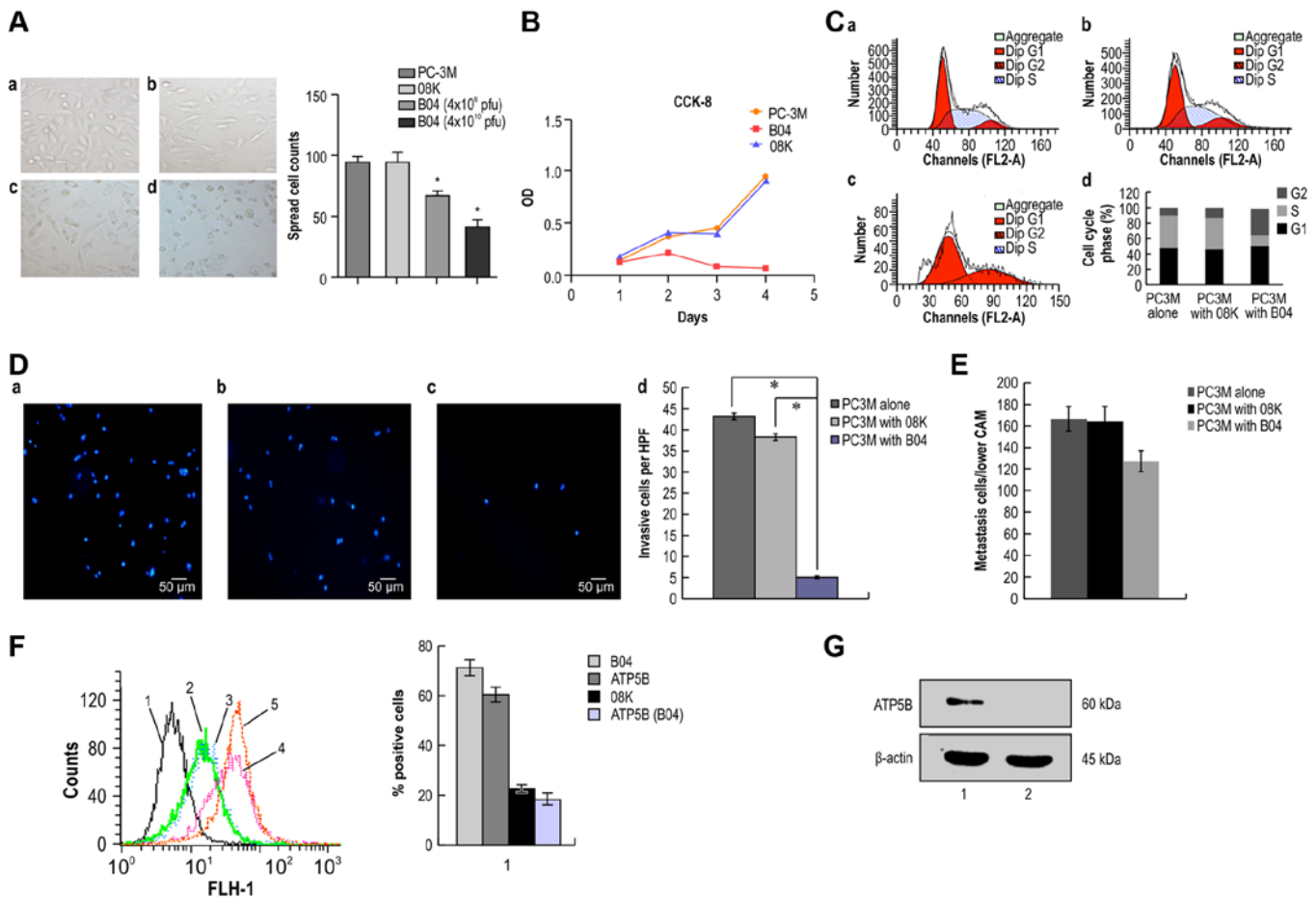


Figure 5. B04 inhibits the proliferation, invasion and metastasis of PC-3M cells by targeting the cell surface protein ATP5B. (A) Effects of B04 on the spreading of PC-3M cells (magnification, x100). (a) PC-3M cells alone; (b) PC-3M cells with 08K (M13 without a seven-peptide gene sequence); (c) PC-3M cells with a lower concentration of B04; (d) PC-3M cells with a higher concentration of B04. A bar graph showing the spread cell counts of each group is given in the right panel. (B) The inhibition rates were determined by CCK-8 assays. Values are the average of triplicate experiments and are represented as the mean \pm SD. (C) Cell cycle distribution of PC-3M cells *in vitro*. PC-3M cells were treated with B04, 08K, or nothing (PC-3M cells alone) for 24 h, and the fraction of cells in each phase of the cell cycle was evaluated by flow cytometry. (a) PC-3M cells alone as a control; (b) PC-3M cells with 08K as a control; (c) PC-3M cells with B04; (d) cell cycle distribution in each group. (D) Effects of B04 on PC-3M invasion in Transwell assays. Representative photographs (a-c) and quantification (d) are shown. Cell nuclei were stained with Hoechst 33342 (blue). (a) PC-3M cells alone; (b) PC-3M cells with 08K; (c) PC-3M cells with B04 (4×10^{10} pfu). Magnification, x100. (E) Effects of B04 on PC-3M cell metastasis in the chicken embryo chorioallantoic membrane (CAM). PC-3M cells were cultured with B04 or 08K, and 10^5 - 10^6 cells were inoculated onto the CAM. After 50 h of incubation, genomic DNA was isolated, and human Alu sequence PCR amplification was performed to determine the number of metastatic cells in each group. * $P < 0.05$ for comparisons between the two groups. (F) Flow cytometry was used to determine the effects of B04 on ATP5B expression. 1, PC-3M cells incubated with Alexa Fluor 488 IgG (control); 2, PC-3M cells incubated with anti-08K antibodies after pre-incubation with 08K; 3, PC-3M cells were incubated with anti-ATP5B antibodies after pre-incubation with B04 for 24 h; 4, PC-3M cells were incubated with anti-B04 antibodies after pre-incubation with B04; 5, PC-3M cells were incubated with anti-ATP5B antibodies. (G) ATP5B bound to B04. Total proteins from PC-3M and PC-3 cells were separated by SDS-PAGE, transblotted and incubated with excessive amounts of B04. Anti-ATP5B antibodies were then added. β -actin was used as a control. Lane 1, total proteins from PC-3 cells; lane 2, total proteins from PC-3M cells.

of ATP5B was significantly decreased in B04 pretreated cells compared with that in the control group, incubated with blank phage. Specifically, ATP5B expression decreased from $61.68 \pm 3.94\%$ in the PC-3M cells alone group and $65.77 \pm 5.75\%$ in the 08K pre-incubated group to $17.62\% \pm 2.5\%$ in the B04 pre-incubated group ($P < 0.05$; Fig. 5F). Moreover, the binding rate of B04 on PC-3M cells ($71.31 \pm 2.58\%$) was significantly higher than that of 08K ($22.53 \pm 0.94\%$) on PC-3M cells ($P < 0.05$; Fig. 5F).

Finally, we confirmed the binding of B04 and ATP5B using competitive binding assays after SDS-PAGE and transblotting of proteins onto PVDF membranes. The results showed that ATP5B on PC-3M cells were specifically blocked by B04 (Fig. 5G).

Discussion

Treatment failure in patients with prostate cancer can frequently be explained by osseous metastasis and invasion to neighboring organs. Advances in predicting the metastasis of prostate cancer will improve survival rates in patients with prostate cancer. Therefore, in the present study, we aimed to identify novel metastasis-related proteins using PC-3M and PC-3 cells, which exhibit differential levels of malignant behavior, coupled with a 7-mer phage library screening. Using this strategy, we identified B04 as a phage peptide that bound to ATP5B specifically on PC-3M cells. Furthermore, blockade of ATP5B with B04 inhibited malignant behavior such as proliferation and invasion of PC-3M cells. These findings

provide important insights into the use of phage technology for identification of metastasis-associated proteins and shed light on the role of ATP5B in metastatic prostate cancer.

Several strategies have been used for the identification of tumor-associated proteins, including serological analysis of recombinant cDNA expression libraries, ribosome display, tumor-specific antibody cloning and phage antibody libraries (8). In the present study, we used a phage antibody library for screening specific short peptides that could target unique protein expression patterns. Peptides have the advantages of high clonal diversity, small size, rapid binding kinetics, and low immunogenicity as detection probes (16,17). Here, we also used bio-panning with normal prostate cells and PC-3 cells to decrease non-specific binding to PC-3M cells in each round. This analysis identified B04 as a ligand for a metastatic protein on PC-3M cells, and subsequent proteomic analysis with MS/MS identified ATP5B as a B04-target protein. These results highlight the applicability of this methodological strategy in the identification of metastasis-related proteins.

ATP5B is part of the catalytic core of the enzyme complex that catalyzes the rate-limiting step of ATP formation in eukaryotic cells. The F1 portion is extramembranous and constitutes the catalytic core, whereas the F0 portion is largely embedded in the membrane and functions as a proton channel involved in proton translocation (18,19). ATP synthases (including ATP5B) are thought to be localized exclusively on the inner mitochondrial membrane. However, in this study, ATP5B was identified from the membranous fraction of PC-3M cells, which indicated the potential translocation of ATP5B from the inner mitochondrial membrane to the outer cellular membrane. These data were further confirmed using double immunofluorescence staining and immunoelectron microscopy, consistent with previous reports by Chi and Pizzo (7) and Ma *et al.* (20). Additionally, we found that ATP5B was localized to the surface of cells in a specimen from a patient with highly malignant prostate cancer. Our results also suggested that ectopic ATP synthase localized to the caveolae of the cell membrane, with the F1 portion directed into the extracellular space. Some studies have also reported that other subunits of the ATP synthase, such as the α and β subunits of the F1 domain and the β - and δ -subunits of F0, can be found on the outside of the membranes of tumor cells and some types of normal cells, including hepatocytes, keratinocytes, adipocytes, endothelial cells and cardiomyocytes (21-24), suggesting that translocation is possible. The enzyme may therefore be called cell surface ATP synthase or ecto-ATP synthase (ecto-ATPase, ecto-F1-ATPase), and ectopically localized ATP5B may be called ecto-ATP5B.

Ectopic ATP synthase has been reported as a structural element and as an enzyme involved in ATP synthesis and proton transport, particularly in some normal cells. Moreover, ATP synthase on the cell surface has been shown to bind a variety of factors, and the β subunit has been shown to be a target of the hormone enterostatin. F1Fo-ATP synthase on the hepatocyte cell surface is localized in caveolae/lipid rafts and functions as a receptor for HDL apolipoprotein A-I, mediating HDL endocytosis. The entire F1Fo-ATP synthase has activity in the endothelial cell surface, with ability to synthesize ATP and transport protons. Moser and colleagues (25,26) identified endothelial cell surface ATPase as a receptor

for angiostatin, which inhibits vascularization by suppression of endothelial surface ATP metabolism. Following ATP synthesis, intracellular protons are pumped out of the cell to prevent acidosis. When the activity of ectopic ATP synthase is blocked, the proliferation and migration of cells could be inhibited, particularly when the cells were cultured with a low extracellular pH. Notari *et al.* (27) reported that pigment epithelium-derived factor (PEDF) functions as a potent blocker of angiogenesis *in vivo*, inhibits endothelial cell migration and tubule formation, reduces the amount of extracellular ATP produced by endothelial cells, and binds with high affinity to ATP5B on the surfaces of endothelial cells. PEDF also blocks the binding between ATP5B and angiostatin. ATP synthesis products may excite the purinoceptor, which has been reported to induce many biological effects, including endothelial cell proliferation and angiogenesis (28). However, the ectopic expression of ATP5B and its potential roles in malignant cells have not been described in detail. Chi and Pizzo (29) reported that ATP5B is expressed on the surface of tumor cells and that treatment with angiostatin or antibodies against ATP5B inhibits the synthase enzyme, suggesting that the activity of ATP5B is independent of the malignant status of cells. For ectopic ATP5B, its specificity to tumors relies on its increased catalytic activity in acidic and hypoxic microenvironments when compared with normal tissues. Consistent with these above findings, our current results showed that ATP5B translocated from the inner mitochondrial membrane to the outer surface of PC-3M cells and that incubation of PC-3M cells with the short peptide B04 reduced the ectopic expression of ATP5B on the PC-3M cellular membrane. Moreover, the proliferation, invasion and metastasis of PC-3M cells were significantly inhibited by specifically blocking the cell surface protein ATP5B. These results indicated that the translocation and ectopic expression of ATP5B on PC-3M cells may be involved in the invasion and metastasis of prostate cancer.

The signaling pathways through which ectopic ATP5B regulates the biological behavior of PC-3M cells are unclear. In our previous MALDI-TOF/MS studies, we found that ATP synthase and caveolin were upregulated in PC-3M cells. In accordance with studies by Ma and colleagues (20) and Chi and Pizzo (29), the purinergic signaling pathway through P2X and P2Y receptors may function to regulate the cell surface ATP synthase. Thus, the following pathway may be involved in this process. First, with the synthesis of ATP, protons are pumped out of the cells. As autocrine agents in the caveolae, ATP synthesis products may excite the purinoceptor (P2Y) to promote cell proliferation, leading to tumor growth and angiogenesis. Cell surface F1Fo-ATP synthase generates ATP and ADP, which may participate in purinergic signaling through P2X and P2Y receptors. Purinergic signaling is implicated in cell growth, proliferation, chemotaxis, inflammatory responses, hypoxic injury and apoptosis (30-34). P2X receptors are ATP-gated, Ca^{2+} -permeable channels that mediate rapid, non-selective passage of cations (Na^+ , K^+ and Ca^{2+}), resulting in an increase in intracellular Ca^{2+} (35). P2Y receptors are G-protein-coupled receptors that regulate cell proliferation through various pathways (36). However, the mechanistic basis of the potential roles of ectopic ATP5B pathways in cancer metastasis is still unclear.

In summary, using a short peptide, B04, identified from screening of a phage peptide library, we identified a metastasis-related protein, ATP5B, located on the cellular surface of PC-3M cells. Ectopic ATP5B was critical for the proliferation, invasion and metastasis of PC-3M cells, and may be a potential biomarker or therapeutic target in highly metastatic tumors. However, the mechanisms through which ATP5B translocates to the cellular membrane of highly metastatic prostate cancer cells and the potential effects of this protein on the metastatic potential of prostate cancer need to be examined more fully in future studies.

Acknowledgements

We thank Dr F. William Orr for his critical suggestions on the organization of the manuscript. The present study was supported by the Jilin Provincial Science and Technology Projects (grant nos. 20150101126JC and 20130102084JC).

References

- Jemal A, Siegel R, Xu J and Ward E: Cancer statistics, 2010. *CA Cancer J Clin* 60: 277-300, 2010.
- Hanahan D and Weinberg RA: Hallmarks of cancer: the next generation. *Cell* 144: 646-674, 2011.
- Kauffman EC, Robinson VL, Stadler WM, Sokoloff MH and Rinker-Schaeffer CW: Metastasis suppression: The evolving role of metastasis suppressor genes for regulating cancer cell growth at the secondary site. *J Urol* 169: 1122-1133, 2003.
- Hanash SM, Madoz-Gurpide J and Misek DE: Identification of novel targets for cancer therapy using expression proteomics. *Leukemia* 16: 478-485, 2002.
- Gao J, Gao Y, Ju Y, Yang J, Wu Q, Zhang J, Du X, Wang Z, Song Y, Li H, *et al*: Proteomics-based generation and characterization of monoclonal antibodies against human liver mitochondrial proteins. *Proteomics* 6: 427-437, 2006.
- Liu B, Huang L, Sihlbom C, Burlingame A and Marks JD: Towards proteome-wide production of monoclonal antibody by phage display. *J Mol Biol* 315: 1063-1073, 2002.
- Chi SL and Pizzo SV: Cell surface F1Fo ATP synthase: A new paradigm? *Ann Med* 38: 429-438, 2006.
- Lu ZJ, Song QF, Jiang SS, Song Q, Wang W, Zhang GH, Kan B, Chen LJ, Yang JL, Luo F, *et al*: Identification of ATP synthase beta subunit (ATPB) on the cell surface as a non-small cell lung cancer (NSCLC) associated antigen. *BMC Cancer* 9: 16, 2009.
- Dowling P, Meleady P, Dowd A, Henry M, Glynn S and Clynes M: Proteomic analysis of isolated membrane fractions from superinvasive cancer cells. *Biochim Biophys Acta* 1774: 93-101, 2007.
- Kim BW, Choo HJ, Lee JW, Kim JH and Ko YG: Extracellular ATP is generated by ATP synthase complex in adipocyte lipid rafts. *Exp Mol Med* 36: 476-485, 2004.
- Hong D, Jaron D, Buerk DG and Barbee KA: Transport-dependent calcium signaling in spatially segregated cellular caveolar domains. *Am J Physiol Cell Physiol* 294: C856-C866, 2008.
- Bae TJ, Kim MS, Kim JW, Kim BW, Choo HJ, Lee JW, Kim KB, Lee CS, Kim JH, Chang SY, *et al*: Lipid raft proteome reveals ATP synthase complex in the cell surface. *Proteomics* 4: 3536-3548, 2004.
- Ribatti D: Chicken chorioallantoic membrane angiogenesis model. *Methods Mol Biol* 843: 47-57, 2012.
- Kariya Y, Kato K, Hayashizaki Y, Himeno S, Tarui S and Matsubura K: Revision of consensus sequence of human Alu repeats a review. *Gene* 53: 1-10, 1987.
- Boyer PD: The ATP synthase - a splendid molecular machine. *Annu Rev Biochem* 66: 717-749, 1997.
- Larimer BM, Thomas WD, Smith GP and Deutscher SL: Affinity maturation of an ERBB2-targeted SPECT imaging peptide by in vivo phage display. *Mol Imaging Biol* 16: 449e58, 2014.
- Goetz M and Wang TD: Molecular imaging in gastrointestinal endoscopy. *Gastroenterology* 138: 828e33.e821, 2010.
- Senior AE: ATP synthesis by oxidative phosphorylation. *Physiol Rev* 68: 177-231, 1988.
- Stock D, Leslie AG and Walker JE: Molecular architecture of the rotary motor in ATP synthase. *Science* 286: 1700-1705, 1999.
- Ma Z, Cao M, Liu Y, He Y, Wang Y, Yang C, Wang W, Du Y, Zhou M and Gao F: Mitochondrial F1Fo-ATP synthase translocates to cell surface in hepatocytes and has high activity in tumor-like acidic and hypoxic environment. *Acta Biochim Biophys Sin (Shanghai)* 42: 530-537, 2010.
- Champagne E, Martinez LO, Collet X and Barbaras R: Ecto-F1Fo ATP synthase/F1 ATPase: metabolic and immunological functions. *Curr Opin Lipidol* 17: 279-284, 2006.
- Jung KH, Song SH, Paik JY, Koh BH, Choe YS, Lee EJ, Kim BT and Lee KH: Direct targeting of tumor cell F₁F₀ ATP-synthase by radioiodine angiostatin in vitro and in vivo. *Cancer Biother Radiopharm* 22: 704-712, 2007.
- Das B, Mondragon MO, Sadeghian M, Hatcher VB and Norin AJ: A novel ligand in lymphocyte-mediated cytotoxicity: Expression of the beta subunit of H⁺ transporting ATP synthase on the surface of tumor cell lines. *J Exp Med* 180: 273-281, 1994.
- Arakaki N, Nagao T, Niki R, Toyofuku A, Tanaka H, Kuramoto Y, Emoto Y, Shibata H, Magota K and Higuti T: Possible role of cell surface H⁺-ATP synthase in the extracellular ATP synthesis and proliferation of human umbilical vein endothelial cells. *Mol Cancer Res* 1: 931-939, 2003.
- Moser TL, Stack MS, Asplin I, Enghild JJ, Højrup P, Everitt L, Hubchak S, Schnaper HW and Pizzo SV: Angiostatin binds ATP synthase on the surface of human endothelial cells. *Proc Natl Acad Sci USA* 96: 2811-2816, 1999.
- Moser TL, Kenan DJ, Ashley TA, Roy JA, Goodman MD, Misra UK, Cheek DJ and Pizzo SV: Endothelial cell surface F1-F0 ATP synthase is active in ATP synthesis and is inhibited by angiostatin. *Proc Natl Acad Sci USA* 98: 6656-6661, 2001.
- Notari L, Arakaki N, Mueller D, Meier S, Amaral J and Becerra SP: Pigment epithelium-derived factor binds to cell-surface F₁-ATP synthase. *FEBS J* 277: 2192-2205, 2010.
- Rumjahn SM, Yokdang N and Baldwin KA, Thai J and Buxton IL: Purinergic regulation of vascular endothelial growth factor signaling in angiogenesis. *Br J Cancer* 100: 1465-1470, 2009.
- Chi SL and Pizzo SV: Angiostatin is directly cytotoxic to tumor cells at low extracellular pH: A mechanism dependent on cell surface-associated ATP synthase. *Cancer Res* 66: 875-882, 2006.
- Schwiebert EM and Zsembery A: Extracellular ATP as a signaling molecule for epithelial cells. *Biochim Biophys Acta* 1615: 7-32, 2003.
- Bodin P and Burnstock G: Increased release of ATP from endothelial cells during acute inflammation. *Inflamm Res* 47: 351-354, 1998.
- Di Virgilio F: Dr. Jekyll/Mr. Hyde: The dual role of extracellular ATP. *J Auton Nerv Syst* 81: 59-63, 2000.
- Ralevic V and Burnstock G: Receptors for purines and pyrimidines. *Pharmacol Rev* 50: 413-492, 1998.
- Wen LT and Knowles AF: Extracellular ATP and adenosine induce cell apoptosis of human hepatoma Li-7A cells via the A3 adenosine receptor. *Br J Pharmacol* 140: 1009-1018, 2003.
- Schwiebert LM, Rice WC, Kudlow BA, Taylor AL and Schwiebert EM: Extracellular ATP signaling and P2X nucleotide receptors in monolayers of primary human vascular endothelial cells. *Am J Physiol Cell Physiol* 282: C289-C301, 2002.
- Burnstock G: Purinergic signaling and vascular cell proliferation and death. *Arterioscler Thromb Vasc Biol* 22: 364-373, 2002.